International Journal of Precision Engineerning and Manufacturing, 2006. 7(3): 66-71

Identification of Human-Generated Forces During Extensor Thrust

Seong-Wook Hong*, PhD
School of Mechanical Engineering, Kumoh National Institute of Technology,
1 Yangho-dong, Kumi, Kyungbuk 730-701, South Korea

Vlad Patrangenaru, BS, **William Singhose**, PhD
School of Mechanical Engineering, Georgia Institute of Technology,
813 Ferst Dr., N.W., Atlanta, GA 30332-0405, USA

Stephen Sprigle, PhD
Center for Assistive Technology and Environmental Access (CATEA), College of Architecture,
Georgia Institute of Technology, 490 Tenth Street, Atlanta, GA 30332-0156, USA

O Number of Pages (including the cover and figures) : 23
O Number of Figures : 6

* Corresponding author
Email address: swhong@kumoh.ac.kr (Seong-Wook Hong)
Phone: +82-54-478-7344, Fax: +82-54-478-7100

Abstract

Background. Involuntary extensor thrust experienced by wheelchair users with neurological disorders may cause injuries via impact with the wheelchair, lead to the occupant sliding out of the seat, and also damage the wheelchair. The concept of a dynamic seat, which allows movement of a seat with respect to the wheelchair frame, has been suggested as a potential solution to provide greater freedom and safety.
Objective. Knowledge of the human-generated motion and forces during unconstrained extensor thrust events is of great importance in developing more comfortable and effective dynamic seats. The objective of this study was to develop a method to identify human-generated motions and forces during extensor thrust events.
Methods. An experimental system was developed to determine the motions of the wheelchair user and the forces at the foot rest. An inverse dynamic approach was employed along with a three-link human body model and a system for measuring human body motion.
Results. Two kinds of experiments were performed: the first experiment validated the proposed model, and the second experiment showed the effects of the extensor thrust speed, the footrest angle, and the seatback angle. The proposed method was tested by a sensitivity analysis, from which a performance index was deduced to help indicate the robust region of the force identification.
Conclusions. A system to determine human-generated motions and forces during unconstrained extensor thrusts was developed. Through experiments and simulations, the developed system was proven effective and reliable.

Relevance

An efficient system to determine human-generated motions and forces during unconstrained extensor thrusts was developed. This system provides beneficial information for the design of personalized dynamic seats for people with high extensor thrust tone.

Key Words: Extensor thrust; wheelchair; dynamic seat; inverse dynamic approach.

1. Introduction

The great advances in medicine and biotechnology allow people with disabilities to live longer and healthier than ever. This has increased the demand for more comfortable, safer and durable wheelchairs. Thus, research on wheelchairs has been concerned with long-term usage, prevention of secondary injury and greater personal freedom [1]. A significant endeavor has also been directed at reducing the necessary effort from family members and care givers. However, there are few reported research results that have been specifically oriented to wheelchairs for people with high extensor thrust.

Extensor thrust is an event when nearly all of the muscles in the body contract simultaneously. As a consequence, the person's body tends to straighten out as shown in Figure 1. Extensor thrust is a symptom usually occurring in people suffering from brain-related diseases such as cerebral palsy. Extensor thrust occurs because the central nervous system is unable to adequately control or supervise the muscles. An often used approach is to highly constrain the patients in their wheelchairs. This is uncomfortable and possibly painful for the constrained occupant.

To provide greater personal freedom and prevent secondary injuries to wheelchair users with high extensor thrust is a challenging problem. Recently, the concept of a "dynamic seat," which allows movement with respect to the wheelchair frame, has been suggested as a potential solution [2]. Some products based on the dynamic seat concept are commercially available [3,4]. However, most of the products appear to be empirically designed only to prevent wheelchair breakage. The ultimate goal of the current study is to develop a method to identify the motion and forces during extensor thrust events. This knowledge will secure the fundamental background for a dynamic seat design.

Attempts at measuring the forces due to extensor thrusts have been made, for example, by measuring the spasticity at the elbow [5], by developing a passive dynamic model of the knee joint affected by spastic paresis [6], and by developing a quantitative measurement of muscle spasticity with the pendulum knee drop test [7]. However, there is little publicly available knowledge regarding the motion and forces during unconstrained extensor thrust events. Since it is very hard to directly measure the human-generated forces, this paper proposes an inverse dynamic approach to indirectly identify the human-generated forces using limited measurements of forces and motion of the occupants.

The inverse dynamic analysis extracts the internal and external forces or moments from measured kinematic responses of the human body segments and some limited set of force measurements. With the help of the inverse dynamic analysis procedure, many researchers have been able to obtain joint forces and moments during biomechanical studies of locomotion, e.g., sit-to-stand, jumping, gait and running. Among these, the study on sit-to-stand movement is most relevant to the current study. Hutchinson, *et al.*, calculated the net forces and torques on human joints using inverse dynamics with measured ground reaction forces and motions during sit-to-stand motions [8]. Biomechanical analysis of sit-to-stand movement by using an inverse dynamic approach has often been performed from a medical point of view, e.g., for a comparison between normal and obese subjects in the joint torques of hip and knee joints [9] and for a comparison between healthy subjects and people with Parkinson's disease [10,11].

There are some significant challenges in the dynamic modeling and analysis of the human body during extensor thrust events in wheelchairs. Unlike biomechanical modeling for locomotion, the dynamics of human body during extensor thrust events are subject to a special set of kinematic constraints because the chair constrains the motion. The lack of information about the reaction forces with the chair makes the problem mathematically indeterminate. The extensor thrust also induces sliding of the body at the edges of seat bottom and seatback of the chair. Mathematical indeterminacy has been an important issue in many biomechanical studies. One of the possible ways to overcome the mathematical indeterminacy is to make the model determinate by ignoring less important variables in the model [e.g., 12]. However, this may require *a priori* knowledge of the forces to be identified. Although optimization techniques have often been employed [13], they may lead to meaningless results unless they are supported by strong physical evidence. Therefore, in this paper, force measurements are made at the foot rest, so as to make the problem mathematically determinate, although efforts are also made to minimize the number of unknown variables.

Inverse dynamic analysis necessitates acceleration measurements. Although some research has sought to obtain direct measurements of acceleration from the human body [14], most investigations have been made with accelerations obtained by numerical differentiation of measured displacements [15,16]. Reducing the effect of noise during the numerical differentiation is an important issue in this approach. In order to minimize the noise induced during the numerical differentiation, this paper takes advantage of kinematic relations. Only one or two measured angular coordinates believed to have low noise are obtained and used to generate the other coordinates based on the kinematic relations.

This paper proposes an efficient method to identify the human-generated forces during extensor thrust events. The paper is confined to the identification of human-generated forces on a rigid chair without the use of restraint belts. An experimental system was developed to measure the motion of the human body and the normal force at the foot rest. The proposed method is capable of identifying the internal and external human-generated forces by using the inverse dynamic analysis with the help of the measurement and the associated digital image processing. The proposed method is demonstrated using simulations and experimental results obtained from people pretending to undergo extensor thrusts.

A preliminary experiment was performed to validate the proposed dynamic model. In this experiment, the human subject intentionally breaks contact with the seat bottom so as to make the system equations mathematically determinate. Additional experiments demonstrate the effects of the extensor thrust speed, the footrest angle and the recline angle of the chair. The proposed method is evaluated as a function of modeling errors. As a result of this sensitivity study, an index function is introduced to help indicate the robustness of the results with respect to modeling error.

2. Dynamic Modeling

2.1 Basic Assumptions

In order to derive a simple yet meaningful dynamic model, several assumptions are made based on careful observation and analysis of an extensor thrust from a mechanical point of view. First, the present study is confined only to a sagittal plane extension motion. Although the extensor thrust event usually includes other effects such as torsional motion, the extension motion is the most common and dominant. Secondly, the human body is assumed to have, without loss of generality, three rigid segments: lower leg, thigh, and upper body (i.e., torso, head and upper extremities). Three joints are considered: ankle, knee and hip. Increasing the number of segments may complicate the model but will not necessarily introduce any further theoretical difficulty other than those discussed with this model later in this paper. Thirdly, the ankle is assumed to be a hinged pivot point with zero torque. Fourthly, the chair is assumed to be rigid. The effect of chair flexibility will be investigated in forthcoming research.

2.2 Equations of Motion

Figure 1(a) shows the schematic model of the human body on a rigid chair. It indicates all the dimensions and coordinates necessary for the model. Figure 1(b) shows the external forces applied to the body, such as gravitational forces and friction forces.

Upon applying Newton's law of motion to each segment, the equations of motion can be obtained as follows:

$$\begin{aligned} m_1\ddot{X}_1 &= F_{aX} - F_{kX} \\ m_1\ddot{Y}_1 &= F_{aY} - F_{kY} - m_1 g \\ I_1^G\ddot{\theta}_1 &= \{F_{aX}\ell_1 + F_{kX}(L_1 - \ell_1)\}\sin\theta_1 - \{F_{aY}\ell_1 + F_{kY}(L_1 - \ell_1)\}\cos\theta_1 - \tau_k \end{aligned} \tag{1a}$$

$$\begin{aligned} m_2\ddot{X}_2 &= -F_{BT}\cos\theta_2 - F_{BN}\sin\theta_2 + F_{bX} - F_{cX} \\ m_2\ddot{Y}_2 &= -F_{BT}\sin\theta_2 + F_{BN}\cos\theta_2 + F_{bY} - F_{cY} - m_2 g \\ I_2^G\ddot{\theta}_2 &= -sign(X_2)F_{BN}\sqrt{X_2^{\,2} + Y_2^{\,2}} + F_{bX}\ell_2\sin\theta_2 - F_{bY}\ell_2\cos\theta_2 + \tau_b - \tau_c \\ &\quad + F_{cX}(L_2 - \ell_2)\sin\theta_2 - F_{cY}(L_2 - \ell_2)\cos\theta_2 \end{aligned} \tag{1b}$$

$$\begin{aligned} m_3\ddot{X}_3 &= -F_{CT}\cos\theta_3 - F_{CN}\sin\theta_3 + F_{hX} \\ m_3\ddot{Y}_3 &= -F_{CT}\sin\theta_3 + F_{CN}\cos\theta_3 + F_{hY} - m_3 g \\ I_3^G\ddot{\theta}_3 &= sign(L_\gamma\sin\theta_r - Y_3)F_{CN}\sqrt{(L_\beta + L_\gamma\cos\theta_r - X_3)^2 + (L_\gamma\sin\theta_r - Y_3)^2} \\ &\quad + F_{hX}\ell_3\sin\theta_3 - F_{hY}\ell_3\cos\theta_3 + \tau_h \end{aligned} \tag{1c}$$

where m_i and $I_i^G, i = 1,2,3$, are the mass and mass moment of inertia for the i-th segment, respectively. The lower case subscripts *a*, *k* and *h* on the forces, F, and torques, τ, denote the ankle, knee and hip joints, respectively. The capital subscripts *B* and *C* denote the corresponding contact points as indicated in Figure 1. The subscripts *T* and *N* represent tangential and normal forces, respectively. All the other parameters which appear in (1) are indicated in Figure 1(a). The tangential forces at the edges of the seat bottom and seatback are friction forces that are proportional to the corresponding normal forces:

$$F_{BT} = u_B F_{BN} \tag{2a}$$

$$F_{CT} = u_C F_{CN} \tag{2b}$$

where u_B and u_C are the friction coefficients at the corresponding contact point, i.e., between the human subject and seat bottom, and between the human subject and seatback, respectively.

The nine equations in (1) contain ten unknown forces and moments, implying that the system is mathematically indeterminate. One of the possible ways to avoid the indeterminacy is to make measurements of one of the unknown variables. In this paper, one unknown force component is measured based on the experimental procedure that will be described in the next section.

Based on the geometric relations, the following kinematic relations can be derived:

$$
\begin{aligned}
&X_1 = \ell_1 \cos\theta_1 - D_1,\ Y_1 = \ell_1 \sin\theta_1 - (L_\alpha - D_2) \\
&X_2 = L_1 \cos\theta_1 + \ell_2 \cos\theta_2 - D_1,\ Y_2 = L_1 \sin\theta_1 + \ell_2 \sin\theta_2 - (L_\alpha - D_2) \\
&X_3 = X_2 + (L_2 - \ell_2)\cos\theta_2 + \ell_3 \cos\theta_3,\ Y_3 = Y_2 + (L_2 - \ell_2)\sin\theta_2 + \ell_3 \sin\theta_3 \\
&\theta_2 = \tan^{-1}\frac{Y_2}{X_2},\ \theta_3 = \tan^{-1}\frac{L_\gamma \sin\theta_r - L_2 \sin\theta_2 + (L_\alpha - D_2 - L_1 \sin\theta_1)}{L_\beta + L_\gamma \cos\theta_r - L_2 \cos\theta_2 + (D_1 - L_1 \cos\theta_1)}
\end{aligned}
\tag{3}
$$

There are eight kinematic constraints but nine coordinates. This leaves only one independent degree of freedom, implying that measurement of one coordinate provides all other coordinates based on the kinematic relations. With the position information, one can obtain the velocity and acceleration data just by analytical differentiation of the kinematic relations given in (3). The kinematic relations are nonlinear, requiring a nonlinear solver. The kinematic relations are very useful for estimating accelerations that are used for inverse dynamic analysis.

3. Force Identification Method Using Inverse Dynamic Analysis

3.1 Generic Equation for the Inverse Dynamic Analysis

Consider the normal and tangential force components at the foot rest, F_{aN} and F_{aT}. The force components at the foot rest can be expressed as follows:

$$
\begin{aligned}
F_{aX} &= F_{aN} \sin\theta_f + F_{aT} \cos\theta_f \\
F_{aY} &= F_{aN} \cos\theta_f - F_{aT} \sin\theta_f
\end{aligned}
\tag{4}
$$

In this case, (1) can be rearranged to give

$$
\underset{9\text{x}10}{[G_0]}\ \underset{10\text{x}1}{\{F_0\}} = \underset{9\text{x}1}{\{Q_0\}} \tag{5}
$$

where

$$\{F_0\} = \{F_{aN}\ F_{aT}\ F_{kX}\ F_{kY}\ F_{BN}\ F_{hX}\ F_{hY}\ F_{CN}\ \tau_k\ \tau_h\ \}^T,$$

$$\{Q_0\} = \{(m_1\ddot{X}_1)\ (m_1 g + m_1\ddot{Y}_1)\ (I_1^G\ddot{\theta}_1)\ (m_2\ddot{X}_2)\ (m_2 g + m_2\ddot{Y}_2)\ (I_2^G\ddot{\theta}_2)\ (m_3\ddot{X}_3)\ (m_3 g + m_3\ddot{Y}_3)\ (I_3^G\ddot{\theta}_3)\}^T$$

$$[G_0] = \begin{bmatrix}
\sin\theta_f & \cos\theta_f & -1 & 0 & 0 & 0 & 0 & 0 & 0 & 0 \\
\cos\theta_f & -\sin\theta_f & 0 & -1 & 0 & 0 & 0 & 0 & 0 & 0 \\
-\ell_1\cos(\theta_1+\theta_f) & \ell_1\sin(\theta_1+\theta_f) & (L_1-\ell_1)\sin\theta_1 & -(L_1-\ell_1)\cos\theta_1 & 0 & 0 & 0 & 0 & -1 & 0 \\
0 & 1 & 0 & -D_{BEX} & -1 & 0 & 0 & 0 & 0 & 0 \\
0 & 0 & 1 & -D_{BEY} & 0 & -1 & 0 & 0 & 0 & 0 \\
0 & \ell_2\sin\theta_2 & -\ell_2\cos\theta_2 & -sign(X_2)\sqrt{X_2^2+Y_2^2} & (L_2-\ell_2)\sin\theta_2 & -(L_2-\ell_2)\cos\theta_2 & 0 & 1 & -1 & \\
0 & 0 & 0 & 0 & 1 & 0 & -D_{CEX} & 0 & 0 & \\
0 & 0 & 0 & 0 & 0 & 1 & -D_{CEY} & 0 & 0 & \\
0 & 0 & 0 & 0 & \ell_3\sin\theta_3 & -\ell_3\cos\theta_3 & L_\delta(\theta_r, X_3, Y_3) & 0 & 1 &
\end{bmatrix}$$

and

$$D_{BEX} = u_B\cos\theta_2 + \sin\theta_2,\ D_{BEY} = u_B\sin\theta_2 - \cos\theta_2,$$

$$D_{CEX} = u_C\cos\theta_3 + \sin\theta_3,\ D_{CEY} = u_C\sin\theta_3 - \cos\theta_3,$$

$$L_\delta(\theta_r, X_3, Y_3) = sign(L_\gamma\sin\theta_r - Y_3)\sqrt{(L_\beta + L_\gamma\cos\theta_r - X_3)^2 + (L_\gamma\sin\theta_r - Y_3)^2}\ .$$

Equation (5) shows that the system is mathematically indeterminate, i.e. the number of unknown forces and moments is greater than the number of equations. Thus, a special condition such as measurement or removal of one unknown variable must be accomplished to directly solve the equation.

3.2 Equation for Model Validation

If there is no contact between the human subject and the seat bottom, then F_{BN} vanishes. In this case, the equations of motion can be rearranged to provide a mathematically determinate equation, which does not require any measurement for the unknown forces to solve: i.e., equation (5) can be rearranged to give

$$\underset{9x9}{[G_1]}\ \underset{9x1}{\{F_1\}} = \underset{9x1}{\{Q_1\}} \qquad (6)$$

where

$$\{F_1\} = \{F_{aN}\ F_{aT}\ F_{kX}\ F_{kY}\ F_{hX}\ F_{hY}\ F_{CN}\ \tau_k\ \tau_h\ \}^T$$

$$\{Q_1\} = \{(m_1\ddot{X}_1)\ (m_1 g + m_1\ddot{Y}_1)\ (I_1^G\ddot{\theta}_1)\ (m_2\ddot{X}_2)\ (m_2 g + m_2\ddot{Y}_2)\ (I_2^G\ddot{\theta}_2)\ (m_3\ddot{X}_3)\ (m_3 g + m_3\ddot{Y}_3)\ (I_3^G\ddot{\theta}_3)\}^T$$

The system matrix $[G_1]$ can be easily derived from $[G_0]$ in (5). The adequacy of the model in the proposed force identification method may be validated with equation (6) by comparing the estimated and measured normal force F_{aN}.

3.3 Equation for Force Identification During Extensor Thrust

Among the unknown forces and moments, the normal force at the foot rest, F_{aN}, is acknowledged as the easiest force component to measure. In this paper, F_{aN} is measured and used to estimate the other forces and moments. If F_{aN} is measurable, equation (5) can be rearranged to give

$$\underset{9x9}{[G_2]}\underset{9x1}{\{F_2\}} = \underset{9x1}{\{Q_2\}} \qquad (7)$$

where

$$\{F_2\} = \{F_{aT}\ F_{kX}\ F_{kY}\ F_{BN}\ F_{hX}\ F_{hY}\ F_{CN}\ \tau_k\ \tau_h\ \}^T$$

$$\{Q_2\} = \{(-F_{aN}\sin\theta_f + m_1\ddot{X}_1)\ (m_1 g - F_{aN}\cos\theta_f + m_1\ddot{Y}_1)\ (F_{aN}\ell_1\cos(\theta_1+\theta_f) + I_1^G\ddot{\theta}_1)$$
$$(m_2\ddot{X}_2)\ (m_2 g + m_2\ddot{Y}_2)\ (I_2^G\ddot{\theta}_2)\ (m_3\ddot{X}_3)\ (m_3 g + m_3\ddot{Y}_3)\ (I_3^G\ddot{\theta}_3)\}^T$$

The system matrix $[G_2]$ is derived from $[G_0]$ in (5). Then, the force vector that includes unmeasured human-generated force components can easily be obtained by solving the linear equation (7).

3.4 Parameters and Kinematic Modeling Error Compensation

The parameters used to describe the human body in the model significantly affect the inverse dynamic analysis results [17,18]. Therefore, accurate parameters are essential to accurate estimation of forces. There are some existing empirical formulae based on cadaver studies and/or computer modeling techniques [17,19]. However, most inertial properties of the human body are still hard to estimate precisely because these properties depend significantly upon

gender, obesity, race and age. In this paper, the regression formulae suggested by Zatsiorsky and Seluyanov [19, 20] have been adopted.

Since the kinematic relations are based on a simple model of the human body, errors may be introduced into estimating kinematic variables. Obviously, the shapes of the back and thigh of each individual human subject also affect the kinematics. The measured angles at the joints are different from those between each segment and the seat. Thus, there are some differences between the theoretical and actual contact points, which are varying along with the change in posture. One of the easy ways to compensate for the error in the thigh segment is replacing the height of the chair by the effective length of chair.

On the other hand, the difference between the measured and estimated values of θ_3 is not changing much during the extensor thrust event. Thus, an easy, approximate compensation for this error is adding a constant angle to the estimated angle θ_3. The moment arm associated with the seatback reaction force is also adjusted since the contact point is not on the line between the hip joint and the mass center of the upper body. The proposed approximations will be proven effective later in this paper. However, in order to obtain more accurate estimates for kinematic variables, it would be helpful to measure and use the curves along the thigh and back.

4. Experiments and Discussion

4.1 Experimental Setup

Figure 2(a) shows the experimental setup that is used to provide measurements of chair forces and human body motion during an extensor thrust event. The experimental system consists of a wheelchair seat with a foot rest, a force plate, a general-purpose digital video camera, a data acquisition system and a PC. The chair has adjustable joint angles and the length of the leg rest is also adjustable. Figure 2(b) shows a sequence of digital image frames taken during an extensor thrust experiment. As can be seen in the figure, markers are attached to the human subject. Human body motion angles are extracted by tracking the markers attached to the human subject using a digital video camera. To synchronize the video measurements with the force measurement, an LED is triggered simultaneously with the starting time of force measurement. At the upper left corner of each frame, the LED distinguishes the starting point of the experiment. There are five markers, which are attached at two joints of interest, the knee and hip joint, as

well as the elbow, shoulder and head. The marker motions are digitally tracked to determine the position data of each link of the human subject.

4.2 Experiment 1: Experimental Validation of the Model

The main goal of this experiment is to establish the validity of the proposed modeling method. An extensor thrust experiment is performed with an intentionally specified motion that breaks contact between the human subject and the seat bottom, so that equation (6) governs this case. Then, there is no need of a force measurement.

The measured angular displacements for such an experiment are shown in Figure 3(a), where the angle θ_3 is computed based on the relative coordinates of the shoulder with respect to the hip joint during the extensor thrust episode. In this analysis, all three angular displacements, θ_1, θ_2 and θ_3, are approximated with fourth-order polynomials and used to compute the other coordinates by using the kinematic relations. Linear and angular acceleration data, which are necessary for the force estimation, are obtained by analytical differentiation of the fourth-order polynomials of angles and the kinematic relations. The nondimensional time is defined as the time divided by the duration of the extensor thrust event.

Figure 3(b) compares the measured and estimated normal forces (F_{aN}) at the foot rest, which are in a good agreement with each other except for some minor fluctuation. The fluctuation in the measured force appears to be caused by an uneven surface and the dynamics of the chair, which rarely affect the human body motion. The accuracy of estimated forces is dependent upon the accuracy of parameters involved in the model. Among others, the friction coefficient is one of the most difficult parameters to be identified. Simulations were performed to see the sensitivity of the results with respect to the friction coefficient between the human subject and the seatback. Figure 3(b) shows the changes in the predicted normal foot force when the friction coefficient, u_C, is changed by ± 0.1 from the nominal value of 0.3. The increase or decrease of friction coefficient shifts the estimation somewhat but still makes the estimation fall into an acceptable region. Thus, it may be deduced that the assumptions introduced to establish the model are acceptable. A detailed sensitivity analysis with respect to modeling errors will be discussed in a later section.

4.3 Experiment 2: Extensor Thrust Test

Experiments are performed to evaluate the effects of extensor thrust speed. In this case, the footrest and seatback angles are set to 15^o and 90^o. Figure 4(a) shows a representative set of measured and estimated angles in this experiment. Figures 4(b) and (c) show identified forces and torques, respectively, while changing the duration of the extensor thrust to approximately 0.8, 1.3 and 2.0 seconds. The lines in the figures represent the average values over three experiments and the error bars indicate the minimum and maximum values at the specified times. The overall pattern of the force and torques does not depend greatly on the speed. Increasing the speed barely affects the force and torque patterns, as well as the change in peak values of the forces and torques. This implies that the gravity forces dominate throughout the event.

To show the effects of the chair configuration, two experiments were made with changing the foot rest and seatback angles. Figures 5(a) and (b) show identified forces and torques from these experiments. Compared with Figure 4, Figure 5 reveals that a change in seatback angle from 90^o to 80^o slightly decreases the normal force at the foot rest but increases the tangential force at the foot rest. This is due to the fact that more tangential force at the foot rest is required to compensate for the increase in horizontal reaction force from the seatback. From Figure 5(a), one can find that the increase of foot rest angle makes it easy to produce horizontal force by increasing the normal foot force. In this case, the tangential foot force is drastically reduced while the normal force is increased. Figure 5(b) shows that the joint torques are also affected by the change of foot rest angle. Overall, the normal force at the foot rest is relatively significant and is the dominant driving force for the extension motion, while the tangential force is less significant but becomes larger as the extension progresses.

4.4 Sensitivity Analysis

Because the proposed method utilizes human-related parameters, which are subject to some amount of uncertainty, it is very important to investigate the robustness of the proposed method with respect to the modeling errors in human parameters. In order to determine the robustness of the proposed identification method, a sensitivity analysis was performed with respect to the human parameters. Among these, masses and mass center locations which are most difficult to estimate or measure are considered. Figures 6(a) and 6(b) demonstrate the variations of the identified forces and torques with the thigh mass, m_2, and the location of mass center of the thigh, ℓ_2, varied 10 % from the nominal values. Overall, the results show that the identified results are not very sensitive to the variation in both cases. In particular, the identification error is less sensitive to the mass center location parameter. However, the identification error due to the thigh mass is relatively significant and is varying with time. The severity of errors appears to

be dependent on the system matrix which is relevant to the dimensions and posture of human body and other seat related parameters. The modeling error sensitivity is extremely high when the system matrix is singular. In order to correlate the system matrix singularity with the sensitivity, the following index is defined:

$$I = \min_i S_i \tag{8}$$

where $S_i, i = 1,2,...,9,$ are singular values of G_2 in equation (7) and defined from the singular value decomposition formula as follows [21]:

$$[G_2] = [U]^T [S][V] \tag{9}$$

Theoretically, every matrix can be decomposed using equation (9), in which the diagonal matrix $[S]$ contains non-negative singular values. If any singular values are zero, then the system matrix is singular. The index in equation (8) is defined so as to represent the degree of non-singularity of the system matrix. The smaller the index is, the more likely the system matrix becomes singular and the identification is more sensitive to modeling errors or noise. Figure 6(c) shows the index for the extensor thrust event corresponding to Figures 6(a) and (b). Comparison of Figure 6(a) and 6(c) reveals that the index becomes small in the region where the variation becomes larger. Therefore, this index provides useful information regarding the robustness of the method for each individual case, or the reliability of the identified results.

5. Conclusions

The knowledge of the human-generated forces during extensor thrust events on wheelchairs is of great importance in the proper design of comfortable, safe, and durable wheelchairs for people suffering from extensor thrust. However, there is little publicly available information regarding the magnitude and time history of human-generated motion and forces during extensor thrust events. This situation exists because the forces and torques are difficult to directly measure. This paper demonstrated a method to measure the motion and determine the associated forces generated by humans during extensor thrust events. An inverse dynamic approach was employed along with a three-link human body model. Measurements at the foot rest were made to compensate for the mathematical indeterminacy of the problem. The experimental system also obtained the angular motion of each human body segment. The proposed method has been

verified through several extensor thrust experiments. As a result of the sensitivity analysis to modeling errors, a reliability index was devised to help indicate the robustness of the identification results. The proposed method will be useful for developing performance specifications and evaluation methods of wheelchair design for people with high extensor thrust.

References

[1] Cooper, R.A., 2001. Advances in wheelchair and related technologies. Medical Engineering & Physics, Vol.23, 3-4, 2001.

[2] Zeltwanger A..P., Brown D., Bertocci G., June 2001. Utilizing computer modeling in the development of a dynamic seating system. Proceedings of the 24th RESNA, Reno, NV, USA.

[3] InterCo GmbH website, http://www.interco-reha.de

[4] Miller's Adaptive Technologies, Product Catalog, 2004

[5] Pandyan, A.D., Price, C.I.M., Rodgers, H., Barnes, M.P., Johnson, G.R., 2001. Biomechanical examination of a commonly used measure of spasticity. Clinical Biomechanics, Vol.16, 859-865.

[6] Lebiedowska, M.K. and Fisk, J.R., 1999. Passive dynamics of the knee joint in healthy children and children affected by spastic paresis. Clinical Biomechanics, Vol. 14, 653-660.

[7] Simon, D. and Foulds, R., 2004. Developing a quantitative measure of muscle spasticity. Proceedings of the IEEE 30th Annual Northeast Bioengineering Conference, Springfield, MA, USA.

[8] Hutchinson, E.B., Riley, P.O. and Krebs, D.E., 1994. A dynamic analysis of the joint forces and torques during rising from a chair. IEEE Trans. Rehabilitation Eng., Vol.2, No.2, 49-56.

[9] Sibella, F., Galli, M., Romei, M., Montesano, Crivellini, A., M., 2003. Biomechanical analysis of sit-to-stand movement in normal and obese subjects. Clinical Biomechanics Vol.18, 745-750.

[10] Mak, M.K.Y., Levin, O., Mizrahi, J., Hui-Chan, C.W.Y., 2003. Joint torques during sit-to-stand in healthy subjects and people with Parkinson's disease. Clinical Biomechanics Vol.18, 197-206.

[11] Mak, M.K.Y., Levin, O., Mizrahi, J., Hui-Chan, C.W.Y., 2004. Reduction of lower limb model indeterminacy by force redundancy in sit-to-stand motion. Journal of Applied Biomechanics, Vol.20, 95-102.

[12] Goossens, R.H.M. and Snijders, C.J., 1995. Design Criteria for the Reduction of Shear Forces in Beds and Seats. Journal of Biomechanics, Vol.28, No.5, 225-230.

[13] Yamaguchi,G.T., Moran, D.W. and Si, J., 1995. A computationally efficient method for solving the redundant problem in biomechanics. Journal of Biomechanics, Vol.28, No.8, 999-1005.

[14] van den Bogert, A.J., Read, L. and Nigg, B.M., 1996. A method for inverse dynamic analysis using accelerometry. Journal of Biomechanics, Vol.29, No.7, 949-954.

[15] Cahouet, V., Luc, M. and David, A., 2002. Static optimal estimation of joint accelerations for inverse dynamics problem solution. Journal of Biomechanics, Vol.35, 1507-1513.

[16] Runge, C.F., Zajac, F.E., III, Allum, J.H.J., Risher, D.W., Bryson, A.E., Jr., and Honegger, F., 1995. Estimating net joint torques from kinesiological data using optimal linear system theory. IEEE Trans. On Biomedical Engineering, Vol.42, No.12, 1158-1164.

[17] Nigg, B.M. and Herzog, W., 1995. Biomechanics of the Musculo-skeletal System, John Wiley & Sons, Inc.

[18] Pataky, T.C., Zatsiorsky, V.M. and Challis, J.H., 2003. A simple method to determine body segment masses in vivo: reliability, accuracy and sensitivity analysis. Clinical Biomechanics, Vol.18, 364-368.

[19] Zatsiorsky, V. and Seluyanov, V., 1985, Estimation of the mass and inertia characteristics of the human body by means of the best predictive regression equations. International Series on Biomechanics, Vol. 5B, 233-239.

[20] de Lava, P., 1995. Adjustments to Zatsiorsky-Seluyanov's segment inertia properties," Journal of Biomechanics, Vol.29, 1223-1230.

[21] Lay, D.C. 1996. Linear algebra and its applications, 2nd ed. Reading, MA: Addison-Wesley.

List of Figures

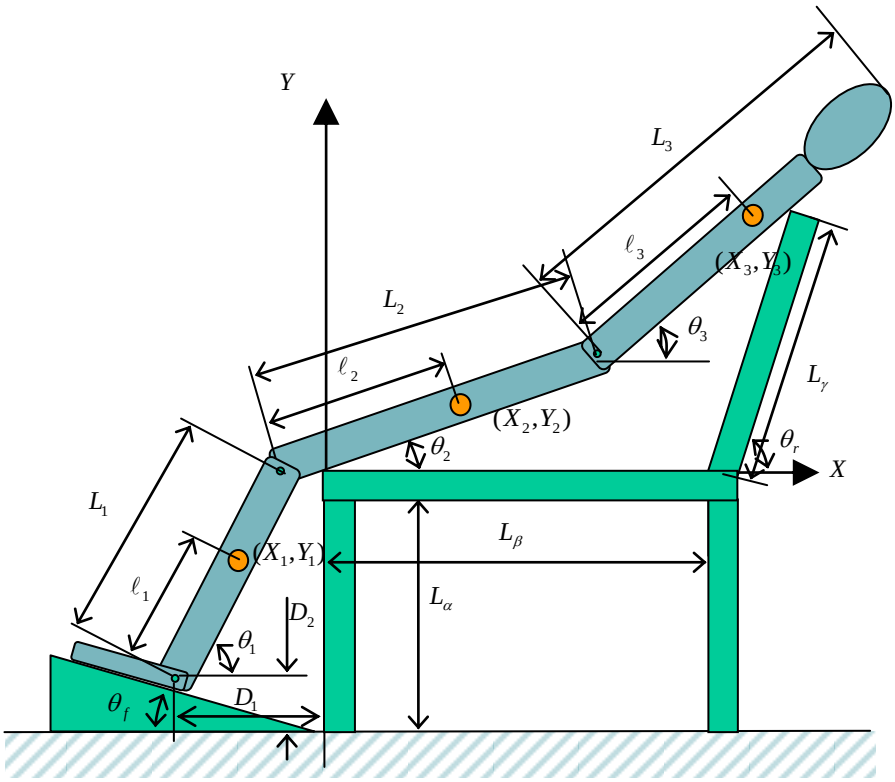

(a) Dimensions and parameters

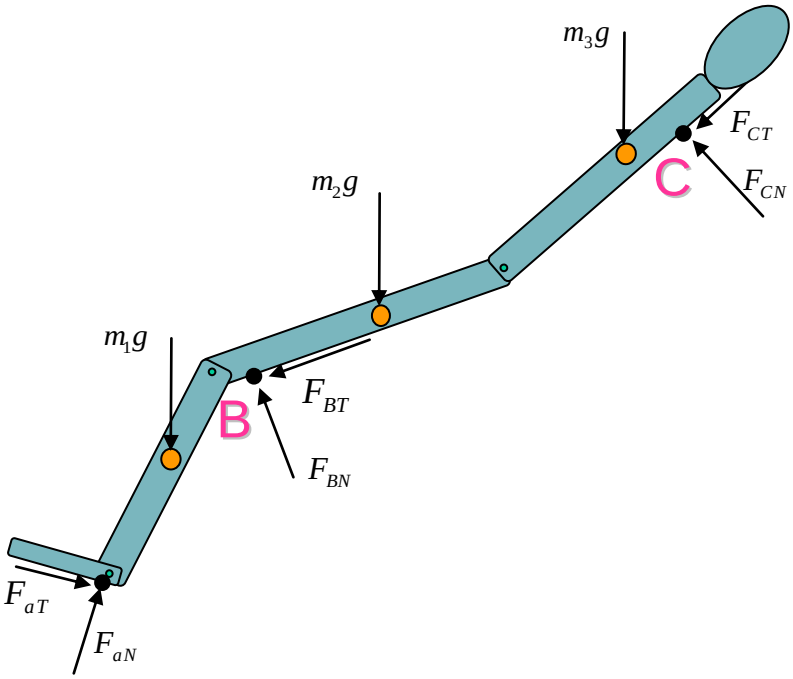

(b) External forces

Figure 1: Schematic model of human body on rigid chair.

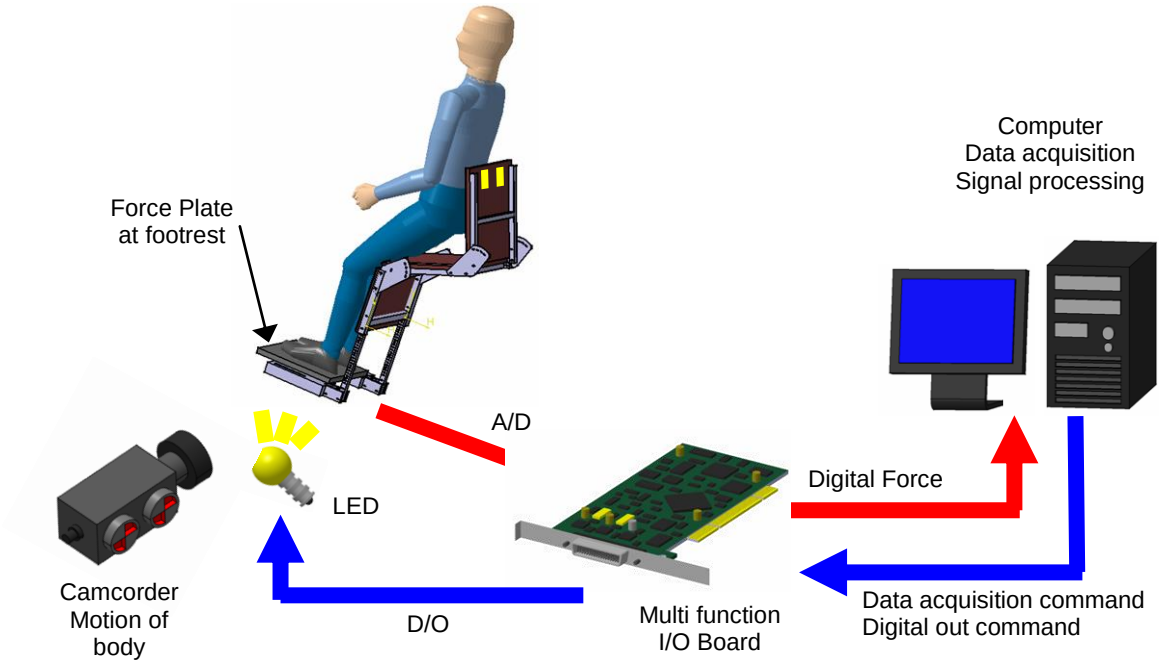

(a) Schematic diagram of the experimental system

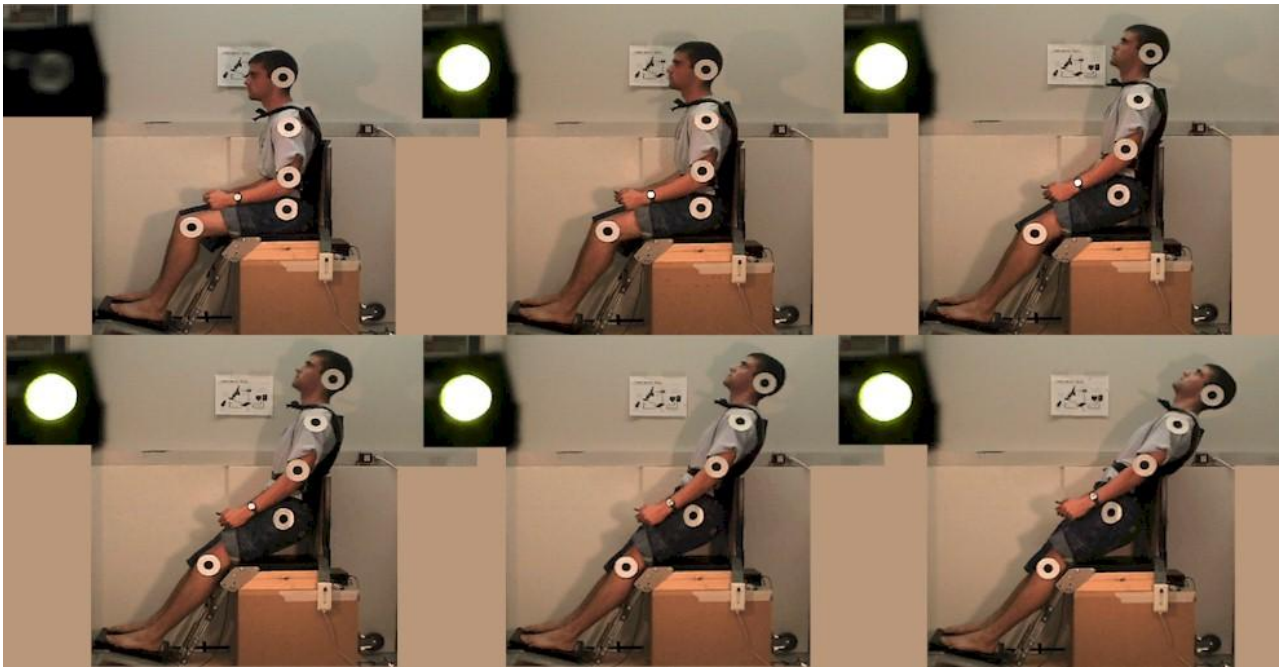

(b) Progression of extensor thrust experiment

Figure 2: Experimental system and illustration of video image from an extensor thrust experiment.

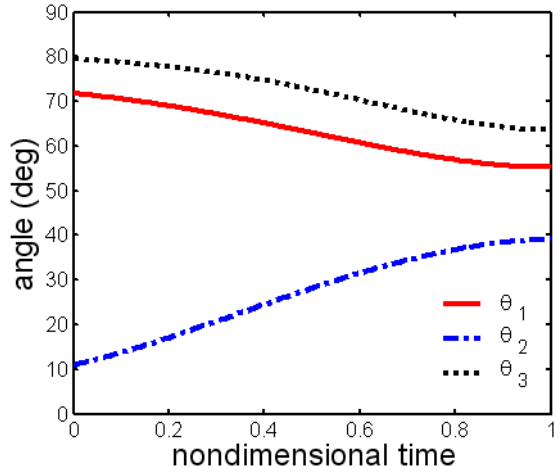

(a) Measured angular displacements

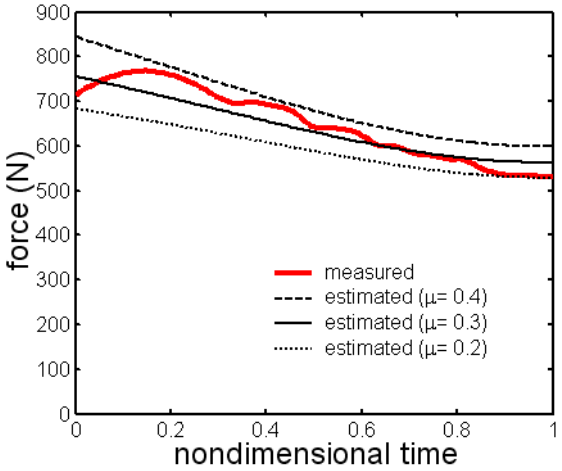

(b) Comparison of measured and simulated normal foot forces

Figure 3: Result from experiment 1: model validation.

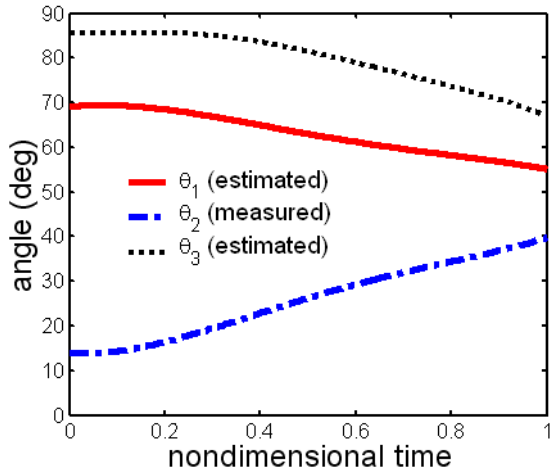

(a) A representative set of measured and estimated angles

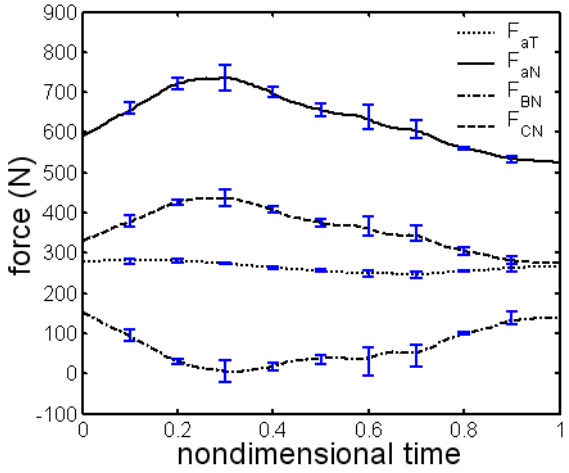

(b) Forces

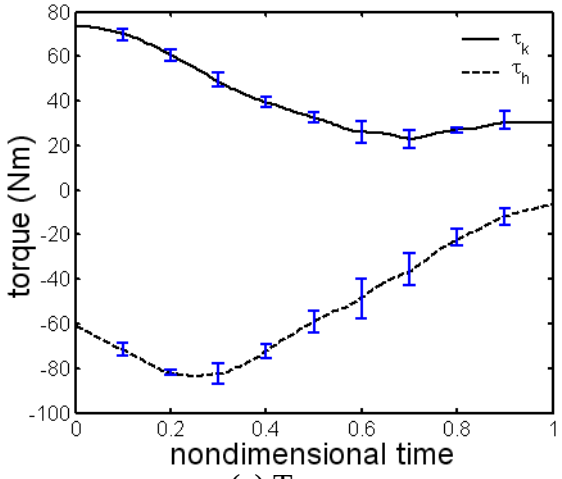

(c) Torques

Figure 4: Identified forces and torques with the duration of extensor thrust event varied: durations = 0.8, 1.3 and 2.0 seconds; foot rest angle = 15 ^{o}, seatback angle = 90^{o}.

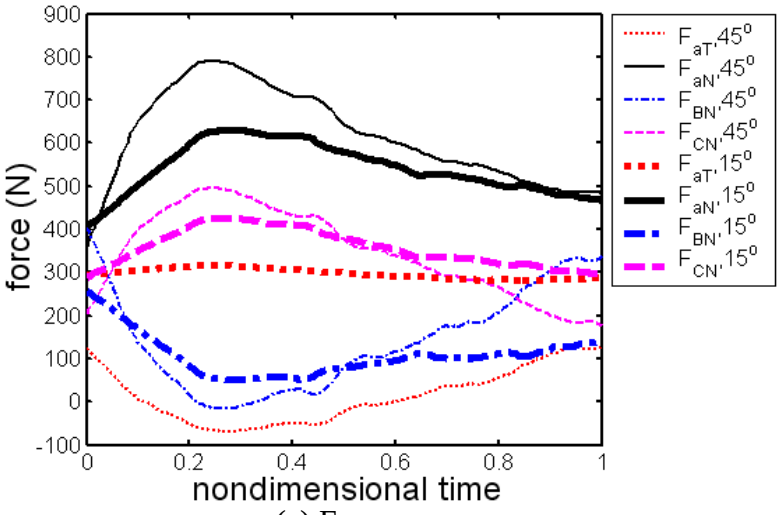

(a) Forces

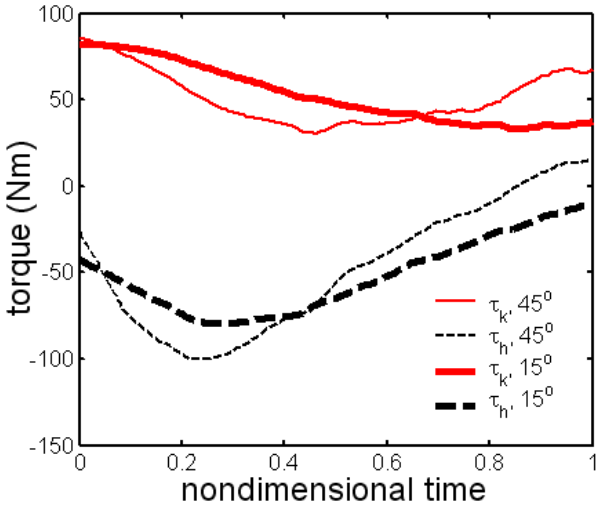

(b) Torques

Figure 5: Forces and torques identified with changing the foot rest angle from 15° to 45°; seatback angle = 80°.

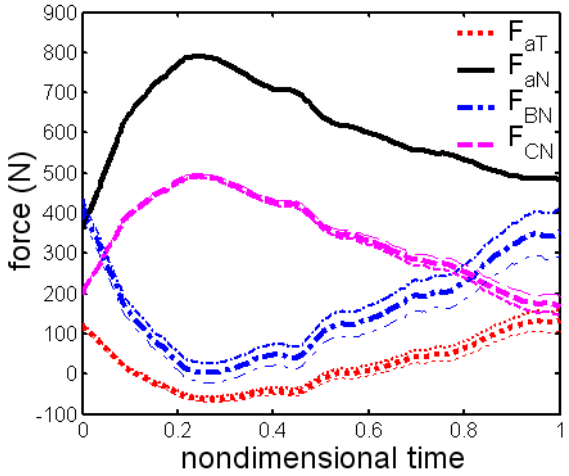

(a) Variation of m_2

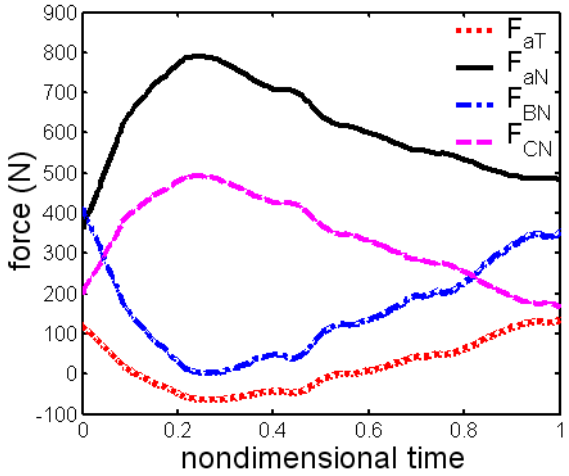

(b) Variation of mass center, ℓ_2

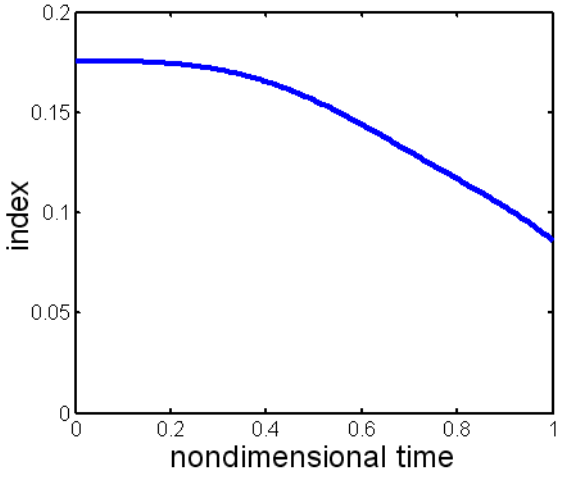

(c) Identification reliability index.

Figure 6: Variation of the identified forces with the mass (m_2) and mass center location (ℓ_2) of the thigh changed by $\pm 10\%$ from the nominal value: the thicker lines are for the nominal values; the footrest and seatback angles are set to 45^o and 80^o. The associated index function is also shown.